Journal of The Electrochemical Society, **147** (10) 3853-3858 (2000)
S0013-4651(00)01-026-0 CCC: $7.00 © The Electrochemical Society, Inc.

Migration-Adsorption Mechanism of Metallic Impurities out of Chemically Amplified Photoresist onto Silicon-Based Substrates

Chin-Cheng Yang,[a] Fu-Hsiang Ko,[a,*,z] Mei-Ya Wang,[b] Tien-Ko Wang,[b] and Shich-Chuan Wu[a]

[a]*National Nano Device Laboratories, National Chiao Tung University, Hsinchu 300, Taiwan*
[b]*Department of Engineering and System Science, National Tsing Hua University, Hsinchu 300, Taiwan*

The radioactive tracer technique was applied to investigate the migration and adsorption behaviors of metallic impurities (*i.e.*, Ba, Cs, Zn, and Mn) out of chemically amplified photoresist onto silicon-based underlying substrates. Two important process parameters, *i.e.*, baking temperatures and substrate types (*e.g.*, bare silicon, polysilicon, oxide, and nitride) were evaluated. Our results indicated that the transition metals (Zn and Mn) have lower migration ratios than alkali metal (Cs) and alkaline earth metal (Ba), irrespective of the substrate types and baking temperatures. The transition metals form stable complexes with the coexisting solvents and/or hydrolysis species in the photoresist layer. The size of the metal complex, the drag force in solvent evaporation, and the baking process were found to have significant effects on impurity migration. A new model, together with the metal migration in the chemically amplified photoresist and the subsequent adsorption onto the underlying substrate, was proposed to explain the pathway of the metal migration. This model could explain the migration ratios of metallic impurities out of the photoresist layer onto the substrate surface.

Manuscript submitted January 7, 2000; revised manuscript received May 16, 2000.

The increasing complexity and miniaturization of modern integrated circuits (ICs) demand a higher device yield and hence lower defect density in the active region of silicon devices.[1] For a deep submicrometer device, metal contamination appearing on the device can cause fatal problems including increasing the leakage current at the p-n junction, decreasing the breakdown voltage of oxide, and reducing the minority carrier lifetime.[2,3] In order to avoid these detrimental effects of metallic contamination, currently the upper limit of metals concentration on the silicon wafer has been set at 10^{10} atoms/cm^2 for manufacturing reliability consideration. Although it is always safer to set stringent specifications, the resulting cost would be extremely high and unnecessary. Therefore, a better understanding of the diffusion route and the behavior of the contaminants introduced into the silicon substrates during device fabrication could be helpful for contamination control and circuit yield promotion.

The control of fabrication processes involved in device manufacturing becomes more and more crucial due to increasing complexity of the materials and tools. Among them, lithography plays a very important role because it is applied repeatedly onto the wafer surface during device manufacturing. Many lithographic models have been developed and applied for the photoresist profile simulation,[4-6] however, the effects of impurity migration in the chemically amplified photoresist are seldom reported. Brown and co-workers[7,8] intentionally contaminated the photoresist with various metals for the evaluation of metal-induced electrical effect. After the lithographic process and photoresist ashing, they applied the optical surface photovoltage method to evaluate the diffusion length of the minority carriers. However, the exact migration ratios and the possible migration mechanism are still unclear for the migration of metallic contaminants out of the photoresist.

The behavior of metallic impurities in chemically amplified photoresist and their migration mechanism is of eminent importance, because proper control of impurity levels in the high-purity photoresist would be very crucial for fast proliferation of chemically amplified photoresist in the IC industry in the coming years. Although it is always safer to demand an unnecessarily high degree of purity for chemically amplified photoresist (10-30 ppb), the resulting cost would be extremely high and unnecessary. The study of the actual amount of migration, the cleaning efficiency, and the electrical effect is beneficial for the establishment of upper limits for each metal.

To evaluate the ratios of metallic impurities migration from chemically amplified photoresist onto the underlying substrate during lithographic processes (*e.g.*, baking), various analytical methods are required for determining the impurities in the photoresist layer and on the surface of the underlying substrate.[9] Methods that have been developed for detecting impurities include graphite furnace atomic absorption spectrometry (GFAAS), inductively coupled plasma mass spectrometry (ICP-MS), total reflection X-ray fluorescence (TXRF) spectrometry, and secondary ion mass spectrometry (SIMS).[10-13] However, these methods suffer from the shortcomings[14-16] of the need to develop the decomposition and pretreatment methods for samples. These methods also require high sensitivity for the instrument and are cumbersome in determining spectroscopic interference. In addition, the required blank control can seriously influence the analytical reliability during measurement.[17,18]

The radioactive tracer technique[19-21] has been proven to be very powerful for studying element migration in materials, environment, and biochemistry. The advantages of this technique include high throughput, ease of operation, interference free from stable isotopes, and a high degree of reliability. Despite the versatility of this technique, however, it is seldom utilized to study impurity migration in the lithographic processes.

Our previous study proposed the radioactive tracer method to investigate the migration of manganese and zinc impurities out of photoresist during the baking process. The simple diffusion model, together with the solvent effect, was used to describe the migration process for metallic contaminants.[22] However, the behaviors of other metallic impurities and the effects of interfacial adsorption were not evaluated.

In this study, the radioactive tracer technique was applied to investigate the migration ratios of different groups of metals (transition and nontransition metal). The relationship between photoresist solvent and migration species was investigated. A correlation function was used to modify the diffusion coefficient for the investigation of the temperature effects. Furthermore, a migration-adsorption model combining the metal migration and chemical equilibrium concept was proposed. The application of the model on impurity migration out of the photoresist and its subsequent reactions onto the underlying substrate was also studied.

Experimental

Materials.—p-Type <100> wafers 15 cm diam were grown with various films (*i.e.*, polysilicon, silicon dioxide, silicon nitride, and nonpassivated or bare silicon control). They were cut into 2 × 2 cm pieces to serve as test samples. These samples were then processed through various lithographic and stripping processes to study the contaminants as introduced in the lithographic process. Carrier-free

* Electrochemical Society Active Member.
z E-mail: fhko@ndl.gov.tw

S0013-4651(00)01-026-0 CCC: $7.00

Table I. Photoresist composition.

Ingredients	Composition (%)	Chemical formula
Propyleneglycol monomethyletheracetate (PGMEA)	<70	$CH_3OCH_2CH(CH_3)OCOCH_3$
Ethyl lactate (EL)	<30	$CH_3CH(OH)COOC_2H_5$
Polyhydroxystyrene derivative	<20	—
Photoacid generator	<1	—
Additive	<1	—
Surfactant	<1	—

radioactive tracers from DAMRI (France) were used in this study. Their compositions were 37 μg/g $^{54}MnCl_2$ (0.838 M Bq/g), 10 μg/g $^{65}ZnCl_2$ (0.857 M Bq/g), 10 μg/g $^{133}BaCl_2$ (0.778 M Bq/g), and 10 μg/g $^{137}CsCl_2$ (0.747 M Bq/g) in 0.1 M hydrochloric acid solution.

The photoresist used in this work was SEPR-401H positive-type photoresist from Shin-Etsu Chemical (Japan). The compositions provided from the vendor are listed in Table I.

This particular photoresist was chosen because it is a popular photoresist for gate and metal layer applications in state-of-the-art ultralarge-scale integrated (ULSI) manufacturing. It can be used in KrF excimer-laser exposure at a wavelength of 248 nm. The photoresist stripper was 1-methyl-2-pyrrolidone (NMP) from E. Merck (Germany).

Film formation process.—To prepare different underlying substrates for study, films of polysilicon and silicon nitride were deposited on various starting silicon wafers by the low-pressure chemical vapor deposition (LPCVD) in a quartz reactor. Polysilicon film was deposited with silane gas (SiH_4) with a flow rate of 60 cm^3/min at 620°C. Silicon nitride film was deposited with a mixture gas of ammonium (130 cm^3/min) and dichlorosilane (SiH_2Cl_2, 30 cm^3/min) at 780°C. Silicon oxide layer was grown by wet oxidation with a mixture gas of hydrogen (8000 cm^3/min) and oxygen (4999 cm^3/min) at 978°C.

Wafers were subsequently cut into 2 × 2 cm pieces to serve as test samples. A photoresist layer was then coated onto each sample. This was accomplished by first holding the test sample on the chuck by vacuum, and then 1 mL of radioactive photoresist was dispensed on the sample surface by pipette. The coating process was performed by spinning at 1500 rpm for 0.5 min. Samples were then split to receive respective baking at 80, 100, and 120°C for a duration of 2 min on a hot plate.

Radioactive tracer experimental procedure.—In order to prepare the radioactive photoresist, one volume of diluted radioactive tracer (0.005 *M*) was mixed with five volumes of photoresist, and the radioactive photoresist solution was well shaken to ensure homogeneous distribution. The radioactive photoresist was then applied to the test sample by the spin-coating process as mentioned previously. After evaporating solvent, the test samples were counted by a high-resolution gamma ray spectrometer. The counting system consists of an HPGe detector coupled with a multichannel analyzer (CANBERRA AccuSpec) and the common electronics. The energy resolution of the system was 2.4 keV at 1332 keV. The intensity of emitted gamma rays for each tracer was monitored at different energy channels as listed in Table II. After counting, the photoresist layer was removed by dipping in a 100 mL NMP solution at 60°C for 5 min and dried on a hot plate. The radioactivity of the impurities left on the wafer was then checked by the same HPGe detection system. The migration ratio of metallic impurities from photoresist to the underlying substrate was determined by the ratio of the time-averaged counts after and before the photoresist stripping.

Table II. Energy and intensity of gamma rays.

Nuclide	Half-life	Energy (keV)	Intensity (%)
Ba-133	10.52 yr	80.997	34.10
		276.398	7.16
		302.853	18.33
		356.017	62.05
		383.851	8.94
Cs-137	30.00 yr	661.66	85.21
Zn-65	244.26 days	1115.546	50.60
Mn-54	312.12 days	834.848	99.98

Results and Discussion

Migration ratios of metallic impurities.—Since the chemically amplified photoresist layer after baking is an amorphous polymer, our previous paper used a diffusion model to predict the behaviors of Mn and Zn in the photoresist layer and in the underlying substrate.[22] This is based on the fact that the concentration of metallic impurities in the photoresist layer is higher than in the substrate immediately after coating the photoresist. During the baking process, the metallic impurities begin migration toward the substrate. However, for the precise description of the metal migration near and onto the substrate, various possible mechanisms including adsorption on the substrate surface, chemical reaction with the substrate surface, diffusion, solubility, precipitation, and gettering may be used to elucidate the migration process.[23-26]

Figures 1-4 depict the migration ratios against baking temperatures for Ba, Cs, Zn, and Mn impurities at each substrate. The results for Cs, Zn, and Mn are somewhat different from our previous reports[11,22] due to the difference in experimental procedure. In this study, the wafer is directly baked after stripping the photoresist layer with NMP solvent, while our previous report is obtained from first water dipping and then baking. In this work, the obtained (percent-

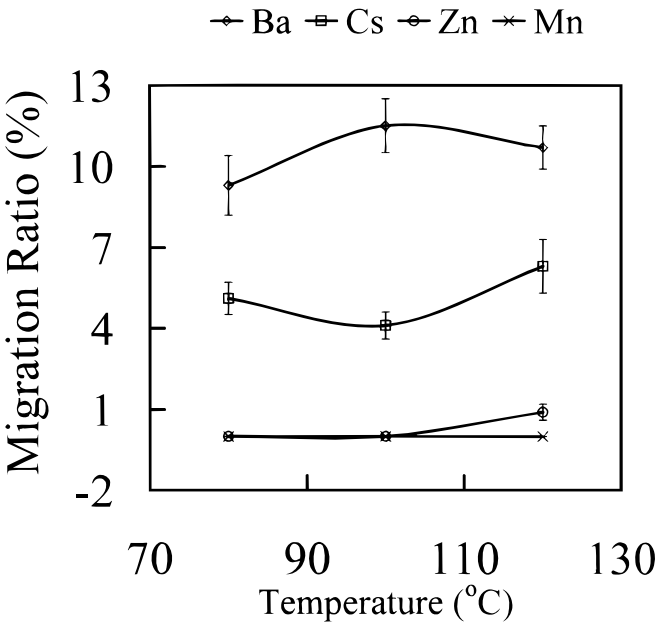

Figure 1. The migration ratios (n = 3) of Ba, Cs, Zn, and Mn impurities *vs.* temperature for bare silicon substrate.

S0013-4651(00)01-026-0 CCC: $7.00

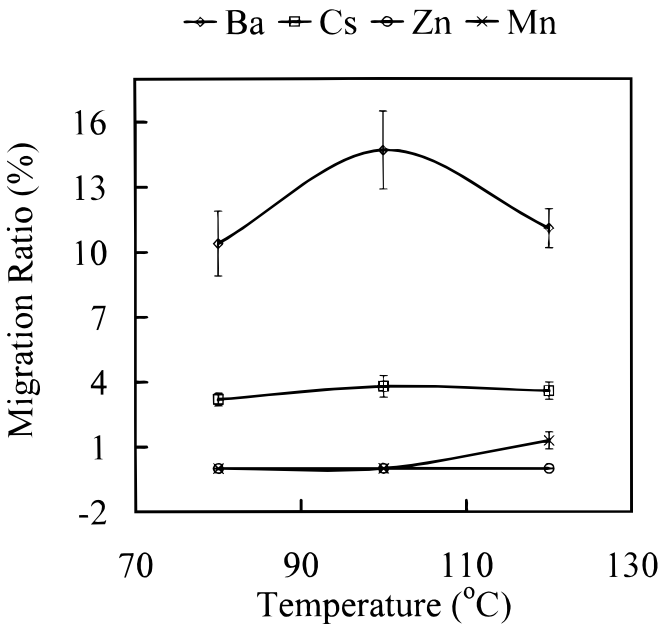

Figure 2. The migration ratios (n = 3) of Ba, Cs, Zn, and Mn impurities *vs.* temperature for polysilicon substrate.

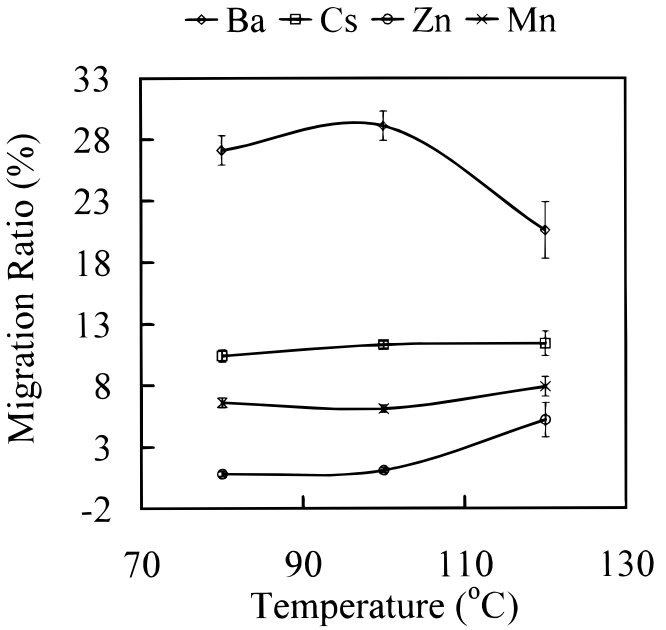

Figure 4. The migration ratios (n = 3) of Ba, Cs, Zn, and Mn impurities *vs.* temperature for silicon nitride substrate.

age) migration ratios can be classified into two groups from Fig. 1-4. The first group with lower migration ratios includes Zn and Mn; whereas the second group of Ba and Cs has comparatively higher migration ratios. This trend implies the transition metals (Zn and Mn) have lower migration ratios than the alkali metal (Cs) and alkaline earth metal (Ba). What are the reasons for the different behaviors? Considering only the effect of ionic radius[27] for the metallic impurity (in Table III), the Cs and Ba with higher ionic radius will face high retardation. Therefore, the migration ratios of Cs and Ba would be expected to be lower. However, as shown in Fig. 1-4, the experimental results do not follow this prediction. Although ionic radius has been ruled out as the major reason in predicting the migration ratio, another possibility remains to be considered. Based on the description of Table I and the preparative procedure of radioactive photoresist, the major solvents in the photoresist layer are propyleneglycol monomethyletheracetate (PGMEA), ethyl lactate (EL), and water. These solvents may have some effect on the migration ratios.

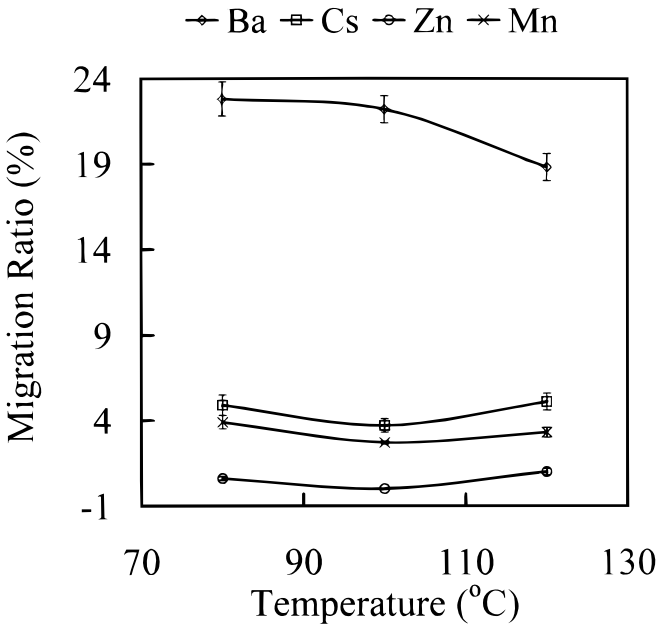

Figure 3. The migration ratios (n = 3) of Ba, Cs, Zn, and Mn impurities *vs.* temperature for silicon dioxide substrate.

The water is introduced in the preparation of tracer contained photoresist. Considering only the hydration effect of water, the metallic impurities become $M(H_2O)_x^{n+}$. The size of various hydration species is also similar, hence the migration ratios should not show significant difference. Because of this, the other solvents (*i.e.*, PGMEA and EL) should play an important role in affecting the migration ratios. This argument is also supported by the boiling point of the solvents: PGMEA and EL have higher boiling points (146 and 154°C, respectively) than water (100°C). Therefore after the normal baking process (100-110°C), the remaining water is limited.

The chemical reactions (Reactions 1 and 2) used for the explanation of the solvent effect on the migration ratios for metallic impurities are expressed as follows

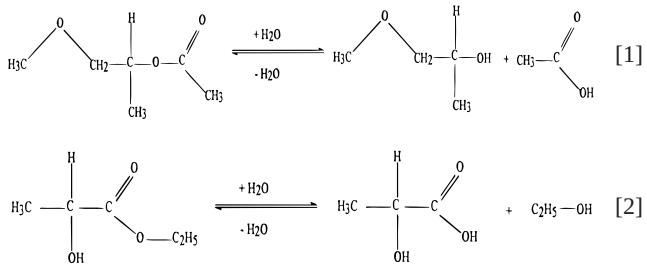

PGMEA and EL are known as the esters. Because the photoacid generator in photoresist can release acid during the baking process, it can act as the catalyst for the hydrolysis of the PGMEA and EL (Eq. 1 and 2). The products of the hydrolysis reaction are acid and alcohol. The esterification and hydrolysis reactions are in equilibrium with each other. Based on the prediction of coordination chemistry, the solvent and hydrolysis products are favored to coordinate with transition metals (*e.g.*, Zn and Mn) through the acetate and/or hydroxyl groups. The solvents and/or hydrolysis products could not only engage in bonding with the transition metals but also form a stable ring complex with polydentate ligands (especially for the EL). Therefore, the transition metals seem to have a larger size after the coordination reaction than the alkali and alkaline earth metals.[28,29] The motion of coordinated complexes shows higher resistance (hin-

S0013-4651(00)01-026-0 CCC: $7.00

Table III. Some properties for the metallic impurities.

	Ba	Cs	Zn	Mn
Atomic number	56	55	30	25
Electron configuration	[Xe] $6s^2$	[Xe] $6s^1$	[Ar] $3d^{10}4s^2$	[Ar] $3d^5 4s^2$
Ionic radii (Å)	1.46 (Ba^{+2})	1.81 (Cs^{+})	0.74 (Zn^{+2})	0.8 (Mn^{+2})
Electronegativity	0.89	0.79	1.65	1.55

drance) within the amorphous polymer layer, which leads to the lower migration ratios.

As can be seen for Ba and Cs from Fig. 1-4, the Ba has significantly higher migration ratios than Cs, irrespective of the substrates. The observation suggests most Ba impurities in the photoresist layer may still exist in the form of free ion, while Cs is in the form of water hydration. The comparatively small size of Ba can lead to higher migration during baking. Experimental results indicate that Ba atoms migrate to the substrate surface during the baking via a diffusion process. Such a metal migration process causes surface contamination, deteriorates device performance, and reduces yield. We believe that the same process occurs virtually at any metal contamination existing in photoresist. Therefore, it is vital to understand the mechanism for controlling metal migration during lithography by continuing this study.

The temperature effect on the migration of metallic impurities—In lithography, soft-baking (usually on a hot plate) can remove most solvents. The solvent gradually evaporates away from the photoresist layer, while metallic impurities in any chemical form begin to diffuse toward the substrate. Theoretically, the temperature-control diffusion can be simply described by the diffusion coefficient (D) and diffusion length (L)

$$D = D_0 \exp \frac{-Q}{kT} \quad [3]$$

$$L = \sqrt{Dt} \quad [4]$$

where D_0 is the pre-exponential factor dependent on the vibration frequency of metallic impurity in the layer and independent of the baking temperature, T is the bake temperature (in kelvin), Q is the energy for activation, k is the Boltzmann constant, and t is the bake time.

It should be noted from Eq. 3 and 4 that higher baking temperature increases the diffusion coefficient and diffusion length. Therefore, without the consideration of other factors, the migration ratios should increase with temperature. It is interesting to observe that the migration ratios did not follow this prediction as baking temperature was elevated from 80 to 120. The observation indicates that Eq. 3 needs to be modified. In order to avoid the discrepancy, a correlation function, $f(T, t)$, is used to modify Eq. 3

$$D = f(T, t) D_0 \exp \frac{-Q}{kT} \quad [5]$$

where $f(T, t)$ is dependent on heat-transfer type (*e.g.*, hot plate, infrared-red, or oven method), heating time, solvent evaporation, and the structure of metallic impurity (*e.g.*, free ion, hydration species, or complex) and photoresist layer.[22]

Table IV. The thickness of photoresist layer for various baking temperatures.

	Bare Si (Å)	Polysilicon (Å)	Silicon oxide (Å)	Silicon nitride (Å)
80°C	8141	8195	8036	8200
100°C	7366	7751	7672	7734
120°C	7177	7344	7205	7358

The differentiation of the diffusion coefficient (in Eq. 5) with temperature can be expressed by the following

$$\frac{\partial D}{\partial T} = D_0\left(\exp \frac{-Q}{kT}\right)\left(\frac{\partial f}{\partial T}\right) + fD_0\left(\exp \frac{-Q}{kT}\right)\left(\frac{Q}{kT^2}\right) = D\left(\frac{1}{f}\frac{\partial f}{\partial T} + \frac{Q}{kT^2}\right) \quad [6]$$

Table IV lists the thickness of photoresist layer at various baking temperatures, showing the thickness decrease with temperature for any substrate. Taking the layer density into consideration, the photoresist layer would become more dense when elevating the baking temperature. The higher baking temperature also induces a higher evaporation rate for residual solvents, therefore, the drag force of solvent evaporation on migration of metallic impurities becomes larger. The metal impurity migrated across the photoresist layer is reduced, especially at higher temperature; hence, the term $\partial f/\partial T < 0$. This argument indicates that the correlation function $1/f\,\partial f/\partial T$ term in Eq. 6 is negative, while the other term Q/kT^2 is positive, whatever the baking temperature and substrate type. Here, the change of migration ratios with temperature can be classified into four types, as shown in Fig. 5. Type I describes the condition when

$$\left|\frac{1}{f}\frac{\partial f}{\partial T}\right| < \left|\frac{Q}{kT^2}\right|$$

the migration ratio increases as the temperature rises. Type II appears when

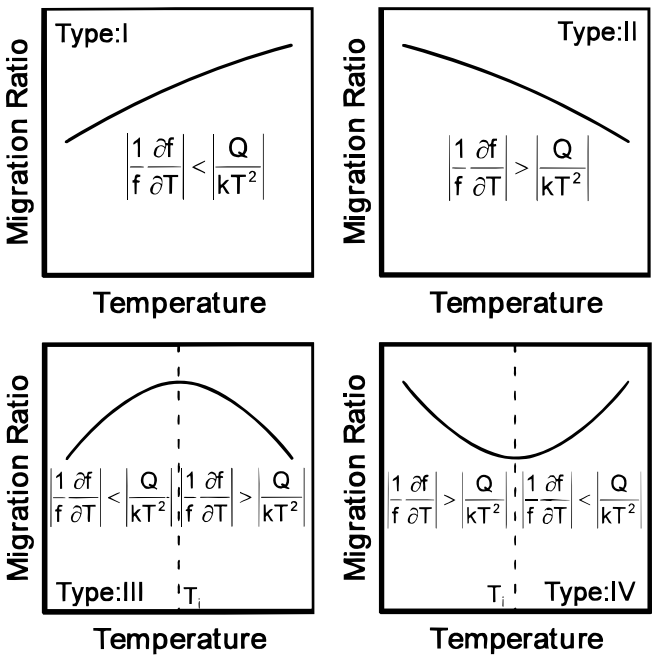

Figure 5. Four types of impurity migration in a polymer layer.

S0013-4651(00)01-026-0 CCC: $7.00

$$\left|\frac{1}{f}\frac{\partial f}{\partial T}\right| > \left|\frac{Q}{kT^2}\right|$$

the migration ratios decrease as temperature rises. Type III has the crossover temperature (T_i) at which

$$\left|\frac{1}{f}\frac{\partial f}{\partial T}\right| = \left|\frac{Q}{kT^2}\right|$$

In the temperature region when $T < T_i$ the tendency of migration ratio behaves like type I; whereas, when $T > T_i$, it behaves like Type II. Type IV also has the crossover temperature, but it shows the opposite tendency as compared with Type III.

Based on this migration model for metallic impurity in a chemically amplified photoresist layer, the results in Fig. 1-4 can be realized. The tendency of Ba migration for substrates of bare silicon, polysilicon, and silicon nitride can be attributed to type III, whereas for substrate of silicon oxide, it belongs to type II. The tendency of Cs migration for substrates of bare silicon and silicon oxide can be attributed to type IV, whereas for substrates of polysilicon and silicon nitride, it belongs to type III and type I. The tendency of Zn migration for substrates of silicon oxide and silicon nitride can be attributed to type IV, whereas for substrates of polysilicon, it belongs to type I. The tendency of Mn migration for substrates of bare silicon and silicon nitride can be attributed to type I, whereas for substrates of silicon oxide, it belongs to type IV. The migration ratios for Mn in polysilicon substrate, Zn in bare silicon substrate are near null for any temperatures. This can be attributed to the migration hindrance in the polymer layer and the drag force of solvent evaporation.

The migration-adsorption model.—Considering the metallic impurity migrating toward the substrate, the migration-adsorption model is first proposed to describe the behavior. Basically, the metallic impurity in the bulk region and interface region as illustrated in Fig. 6 should be considered. In the bulk region, the temperature and solvent effects are the controlling factor. The higher baking temperature induces the higher diffusion toward the substrate, while the coexisting solvent evaporates in the opposite direction. Therefore, according to the description in the previous section, the metallic impurity would have complex behavior in the bulk region.

In the interface region, the original metallic impurity and the impurity migrated from the bulk region may interact with the substrate. There are three possible mechanisms that can be used to explain the interaction. The first is related to electronegativity.[30] Because the Ba, Cs, Zn, and Mn have lower electronegativity when compared with silicon (*i.e.*, 0.89, 0.79, 1.65, and 1.55 on the Pauling scale[31] for Ba, Cs, Zn, and Mn, respectively, compared with 1.9 for silicon), cations of Ba, Cs, Zn, and Mn cannot be neutralized by taking an electron from silicon. Therefore, electronegativity is eliminated as the interaction mechanism. The second mechanism is related to the formation of metal silicates. However, the formation of metal silicates often requires temperature higher than 800°C,[24] it is not accessible at the lower temperature used for photoresist baking.

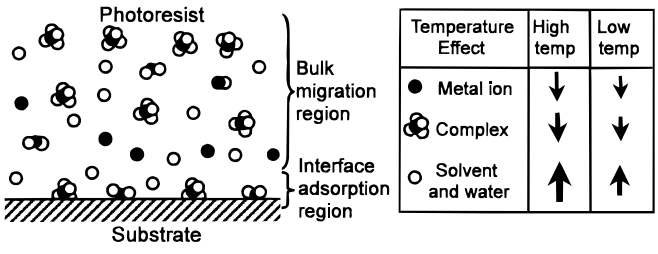

Figure 6. The migration-adsorption model for the metallic impurity transported from the bulk migration region (photoresist) onto the interface adsorption region (substrate). The direction and length of the arrow on the right represents the migration direction and rate. Higher length for the arrow represents a higher migration rate

The third mechanism considers the effect of surface adsorption for the metallic impurities.[23,24] Because the water in the photoresist layer can induce native oxide formation, it can be assumed that the substrate surface is covered with silanol group (SiOH). The silanol group can react with the metallic impurity based on the following equation

$$\text{Si-OH} + M^{n+} \leftrightarrow \text{SiOM}^{(n-1)+} + H^+ \quad [7]$$

If the chemical reaction reaches equilibrium, the equilibrium constant (K) for the reaction can be expressed as

$$K = \frac{\sigma_{\text{SiOM}^{(n-1)+}}[H^+]}{\sigma_{\text{SiOH}}[M^{n+}]} \quad [8]$$

where $[H^+]$ and $[M^{n+}]$ are volume concentrations for the generated acid and metallic impurity in the interface region, while $\sigma_{\text{SiOM}^{(n-1)+}}$ and σ_{SiOH} are surface concentrations.

From Eq. 8, the concentration of surface metal adsorption can be rewritten as

$$\sigma_{\text{SiOM}^{(n-1)+}} = \frac{K\sigma_{\text{SiOH}}[M^{n+}]}{[H^+]} \quad [9]$$

It clearly demonstrates that the amount of adsorbed metal is dependent on the surface density of the adsorption sites (silanol group), the equilibrium constant of the reaction, the acid concentration in the interface region, the concentration of metallic impurity in the interface region, and the baking temperature. Furthermore, the amount of adsorbed metal is directly related to the migration ratios. Higher surface adsorption site concentration, higher metallic concentration in the interface region, and the more basic conditions lead to the higher migration ratios for metallic impurity.

Application of migration-adsorption model.—In the previous section, we proposed the migration-adsorption model to describe the behavior of metallic impurity existing in the photoresist layer. The model demonstrates that the migration ratios are controlled by two factors. The first one is the amount of metals migrating from the bulk region into the interface region. The second one is the surface adsorption predicted by Eq. 9 in the interface region. The new proposed model is consistent with the experimental results in Fig. 1-4.

As mentioned previously, the migration rate of transition metals is lower than the alkali and alkaline earth metals in the bulk region. The transition metal has lower concentration in the interface region, and the term $[M^{n+}]$ in Eq. 9 is lower for transition metals. In the interface region for the same sample, the terms of σ_{SiOH} and $[H^+]$ are the same. For the equilibrium constant (K), Loewenstein and coworkers[23,24] have shown that the attraction between the metal ion and adsorbed site influenced the equilibrium constant. Because the alkali and alkaline earth metals have larger charge-to-radius ratio than transition metal complexes, they show a higher attraction force with the surface silanol group. According to this reasoning, the equilibrium constant of transition metals is lower than alkali and alkaline earth metals in Eq. 9. Taking the above reasons into consideration, the transition metal has lower surface metal adsorption. Thus, the migration ratios, appearing in Fig. 1-4, can be explained and predicted with the proposed migration-adsorption model.

Conclusion

The mechanism and modeling of migration of metallic impurities in a photoresist layer and adsorption onto the substrate surface have been successfully proposed to describe the behavior of baking effects ranging from 80 to 120. Solvent properties and baking temperature play an important role in the migration process. Transition metals (Zn and Mn) form a complex with solvent and/or a hydrolysis product during the baking process. The coordinated complex shows higher resistance through the motion in the photoresist layer, which leads to the lower migration ratios. The correlation function, used to modify the diffusion coefficient, can describe the different trends of temperature effect on migration ratio.

S0013-4651(00)01-026-0 CCC: $7.00

In the proposed migration-adsorption model, the migration of metallic impurity proceeds in two pathways (*i.e.*, in the bulk region and in the interface region). In the bulk region, the size and solvent effects influence the migration of metallic impurities. In the interface region, surface adsorption is the mechanism affecting migration ratios.

The equilibrium equation, used to describe the relationship of the concentration of adsorbed surface metal, the equilibrium constant, the surface concentration of silanol groups, the concentration of metallic impurity, and the pH value, is very useful for the elucidation of the migration ratios for Ba, Cs, Zn, and Mn.

Acknowledgments

The authors to thank the National Science Council of Taiwan for financial support for this research through contracts NSC89-2113-M-317-001. In addition, they would also like to thank Professor Kuo-Shen Chen of National Cheng Kung University for valuable comments and technical suggestions regarding this paper.

The National Chiao Tung University assisted in meeting the publication costs of this article.

References

1. S. M. Sze, *VLSI Technology*, p. 623, McGraw-Hill, NY (1988).
2. C. Y. Chang and S. M. Sze, *ULSI Technology*, p. 680, McGraw-Hill, New York (1996).
3. P. J. Ward, *J. Electrochem. Soc.*, **129,** 2573 (1982).
4. F. H. Dill, W. P. Hornberger, P. S. Hauge, and J. M. Shaw, *IEEE Trans. Electron Devices*, **ED-22,** 445 (1975).
5. D. J. Kim, W. G. Oldham, and A. R. Neureuther, *IEEE Trans. Electron Devices*, **ED-31,** 1730 (1984).
6. C. A. Mack, *J. Electrochem. Soc.*, **134,** 148 (1987).
7. S. Brown, P. Ackmann, V. Wenner, and J. Lowell, in *IEEE/SEMI Advanced Semiconductor Manufacturing Conference*, p. 316 (1995).
8. J. Lowell, P. Ackmann, S. Brown, J. Sherry, and T. Hossain, *Proc. SPIE-Int. Soc. Opt. Eng.*, **2725,** 206 (1996).
9. J. S. Crighton, J. Carroll, B. Fairman, J. Haines, and M. Hinds, *J. Anal. At. Spectrom.*, **11,** R461 (1996).
10. G. R. Fuchs-Pohl, K. Solinska, and H. Feig, *Fresenius'*, *J. Anal. Chem.*, **343,** 711 (1992).
11. F.-H. Ko, M.-Y. Wang, and T.-K. Wang, *Anal. Chem.*, **71,** 5413 (1999).
12. M. B. Shabani, T. Yoshihiro, and H. Abe, *J. Electrochem. Soc.*, **143,** 2025 (1996).
13. M. G. Dowsett, R. D. Barlow, and P. N. Allen, *J. Vac. Sci. Technol.*, **B12,** 186 (1994).
14. L. Fabry, S. Pahlke, L. Kotz, and G. Tolg, Fresenius, *J. Anal. Chem.*, **349,** 260 (1994).
15. F.-H. Ko and M.-H. Yang, *J. Anal. At. Spectrom.*, **11,** 413 (1996).
16. R. N. Sah and P. H. Brown, *Microchem. J.*, **56,** 285 (1997).
17. G. Tolg, *Talanta*, **21,** 327 (1974).
18. J. W. Mitchell, *Talanta*, **29,** 1035 (1982).
19. R. J. Borg and G. J. Dienes, *An Introduction to Solid State Diffusion*, p. 255, Academic Press, New York (1988).
20. I. P. Glekas, *Water Sci. Technol.*, **32,** 179 (1995).
21. G. R. Choppin and J. Rydberg, *Nuclear Chemistry*, p. 425, Pergamon Press, Oxford (1980).
22. M.-Y. Wang, F.-H. Ko, T.-K. Wang, C.-C. Yang, and T.-Y. Huang, *J. Electrochem. Soc.*, **146,** 3455 (1999).
23. L. M. Loewenstein and P. W. Mertens, *J. Electrochem. Soc.*, **145,** 2841 (1998).
24. L. M. Loewenstein, F. Charpin, and P. W. Mertens, *J. Electrochem. Soc.*, **146,** 719 (1999).
25. K. Graff, *Metal Impurities in Silicon-Device Fabrication*, p. 7, Springer, Berlin (1995).
26. J.-P. Joly, *Microelectron. Eng.*, **40,** 285 (1998).
27. F. A. Cotton and G. Wilkinson, *Advanced Inorganic Chemistry*, p. 1386, John Wiley & Sons, New York (1988).
28. C. E. Mortimer, *Chemistry*, p. 679, Van Nostrand, New York (1971).
29. G. B. Kauffman, *Coordination Chemistry*, American Chemical Society, Washington, DC (1994).
30. M. Sano, in *Proceedings of the 10th Workshop on ULSI Ultra Clean Technology*, Tokyo, Japan, p. 55, Ultra Clean Society (1991).
31. *CRC Handbook of Chemistry and Physics*, 79th ed., D. R. Lide, Editor, pp. 9-74, CRC Press, Boca Raton, FL (1998).